J. Membrane Biol. 115, 31–40 (1990)

The Journal of
Membrane Biology

ESR Measurement of Time-Dependent and Equilibrium Volumes in Red Cells

Mario M. Moronne, Rolf J. Mehlhorn, Michael P. Miller, Larry C. Ackerson, and Robert I. Macey
Department of Physiology-Anatomy, University of California, Berkeley, California 94720

Summary. Red cell water volumes were measured using ESR methods during transient osmotic perturbation, and under equilibrium conditions. Cell water contents were determined using the spin label Tempone (2,2,6,6-tetramethyl piperidine-N-oxyl) and the membrane impermeable quencher potassium chromium oxalate. With appropriate corrections for intracellular viscosity and changes in cavity sensitivity, equilibrium cell water measured both by electron spin resonance (ESR) and wet minus dry weight methods gave excellent agreement in solutions from 243–907 mOsm. Intracellular viscosities determined from the Tempone correlation times in the same cells gave values ranging from 9–47 centipoise at 21°C.

Osmotically induced transient volume changes were measured using Tempone and an ESR stopped-flow configuration. The Tempone response time was estimated at 17 msec compared to 250–350 msec for normal water relaxations. Nonlinear least square solutions to the Kedem-Katchalsky equations including a correction for the finite Tempone permeability gave 0.029 and 0.030 cm/sec for the osmotic permeability of RBCs in swell and shrink experiments, respectively. In stopped-flow experiments accurate water flux data are obtained very soon after challenging cells and do not require baseline subtractions. These results represent significant improvements over conventional light scattering techniques which necessitate corrections for long lasting optical artifacts (200–300 msec), and baseline drifts.

Key Words erythrocyte · ESR · water · permeability · microviscosity · transport · osmosis

Introduction

Red cell hydration is a key factor regulating erythrocyte deformability (Williams & Morris, 1980), and is thought to play a crucial role in the pathology of sickle cell disease (Bookchin, Balazs & Landau, 1976). Information about the state of red cell hydration at equilibrium and during transient osmotic stress is essential for predicting the response of red cells in environments like the kidney. The flow of water in and out of red cells is thought to depend on the presence of water channels whose existence has been inferred from observations comparing cellular properties with those of lipid bilayers. These include the cell's high permeability to water, low activation energy, and the fact that the osmotic water permeability (P_f) of the red cell is considerably higher than its diffusional water permeability (P_d) (Paganelli & Solomon, 1957; Macey, Karan & Farmer, 1972; Moura et al., 1984). Although each factor is easily explained by the presence of continuous water channels perforating the membrane, it is the comparison of P_f and P_d that provides the compelling argument. Not only does this comparison argue strongly for the channel's existence, the magnitude of the ratio P_f/P_d has implications about channel structure; if water moves through the channel in single file, P_f/P_d equals the number of water molecules residing in each channel (provided proper corrections are applied to adjust for the nonzero water permeability of the bilayer) (Levitt & Subramanian, 1974; Finkelstein & Rosenberg, 1979; Moura et al., 1984).

Given these interpretations, it is important to examine the validity of estimates of both P_f and P_d. Measurements of P_d have been obtained by use of two independent methods, NMR and tracer exchange. Both methods depend on simple physical principles that are well understood, and the results generally show good agreement (Brahm, 1982). In contrast, although P_f has been measured in many laboratories, it is generally based on a single optical method (light scattering, or transmission) which is complicated and not easily understood. Further, the methods generally require the sudden mixture of cells with suspending solutions, a process which results in the introduction of considerable artifacts in the optical signal. Unfortunately, the artifacts decay with a time constant similar to the time constant for water equilibration, making it difficult to extract the signal with complete reliability (Mlekoday, Moore & Levitt, 1983).

In this paper we show that electron spin resonance (ESR) techniques can be used effectively to measure red cell volume transients as well as equilibrium volumes. Earlier studies using the spin probes tempamine and MAL-3 measured changes in the microviscosity of red cells by monitoring the probe correlation times (Daveloose et al., 1983; Morse, 1985). Similar measurements were made on solutions of normal and sickle hemoglobin with and without oxygenation using the probe Tempone (Beaudoin & Mizukami, 1978). Static cell and vesicle volumes have been measured with Tempone and chromium oxalate quencher (Vistnes & Puskin, 1981). Still other studies have used spin probes to measure the internal volumes of vesicle preparations from plant membranes and phospholipids (Mehlhorn, Candau & Packer, 1982) and transient volume fluxes in membrane vesicles (Anzai, Higashi & Kirino, 1988).

These methods are readily adapted for measuring red cell water fluxes under varying conditions of osmotic stress. In addition, when proper attention is given to the changes of spin label spectra in media of high viscosity and reduced water content, red cell equilibrium volumes and internal microviscosities can be determined. The following advantages are obtained using ESR for stopped-flow experiments: (*i*) optical artifacts are eliminated permitting accurate data to be obtained very soon after osmotic challenges without relying on baseline subtractions, (*ii*) effects of changing cell shape and density are essentially eliminated, (*iii*) intracellular microviscosity can be measured simultaneously. For static volume measurements, ESR has the principal advantages of being nondestructive and capable of utilizing packed volumes of cells as small as 3–5 μl in a standard T102 cavity or as low as 0.2 μl using a loop-gap resonator (Hubbell, Froncisz & Hyde, 1987).

Materials and Methods

Most experiments were done using venous blood obtained from healthy volunteers and stored in acid-citrate-dextrose or EDTA as an anticoagulant. Cells were used within hours for static volume measurements, and within three days for kinetics studies. In a few experiments newly expired blood bank blood was used with essentially the same results. Blood was washed three times in buffered saline and the buffy coat carefully removed. All measurements were made at 21° and a pH of 7.4. Sucrose or KCl was used for osmotic control in shrink experiments. Tempone (2,2,6,6-tetramethyl piperidone-N-oxyl) was used for both static and rapid mix experiments. Osmotic activities of solutions were measured using a Wescor vapor pressure osmometer. Cell counts were performed using a Coulter Counter. All chemicals were at least reagent grade.

In most experiments, quenching of the extracellular signal was accomplished with 50–60 mM potassium chromium oxalate plus 50–75 mM KCl or NaCl. In the time scale of typical experiments the chromium oxalate complex appears to be completely impermeant. In addition, this mixture proved to be effective without perturbing normal red cell volumes or shape as monitored by light microscopy. The presence of external chloride is essential to prevent cell shrinkage and cell deformation owing to its comparatively high permeability; without it the chloride gradient promotes a net efflux of KCl. As a result, cells shrink and become echinocytic. To obtain the equivalent degree of quenching with potassium ferricyanide requires at least 150 mM and suffers from the disadvantage of restricting external osmolarities to isotonic values or greater. Furthermore, ferricyanide may oxidize sensitive red cell sulfhydryl groups, and, in fact, treatment with 50 mM appears to convert red cells into echinocytes even in the presence of a like amount of external chloride.

For static volume measurements, samples were prepared by twice pelleting and resuspending the washed blood in isotonic quencher, and then packed one more time at 12,000 × *g*. Packed cell samples from 390–410 mg were carefully weighed into microcentrifuge tubes and suspended in solutions of varying osmolalities to 2-ml final volumes. Twenty μl of 20 mM Tempone was added to each sample just prior to taking its spectrum. The cell suspensions were immediately divided for ESR and wet minus dry weight measurements (wet-dry). In addition, supernatants from each cell suspension were analyzed by osmometry to determine their final equilibrium osmolalities. The ESR spectra were completed within 2 min after adding the Tempone. This is important because reducing components in red cells lead to a slow decay of the signal (half time ~1 hr). The effect can be largely inhibited by the addition of 5 mM ferricyanide to the suspension media which reoxidizes the reduced probe.

Wet and dry weight measurements were made with slight modifications to the micromethod of Adorante and Cala (1987). In brief, packed cells were weighed, then resuspended in distilled water and the cell solids precipitated with $ZnSO_4$ followed by lithium hydroxide treatment. The supernatant was removed and the sample dried in an 80°C oven until they reached constant weights (18–24 hr). The difference between the wet and dry weights was taken as the cell water after correction for trapped volume. The trapped volumes were evaluated using radioactive sucrose and by ESR using an impermeable nonbinding cation spin probe CAT1(trimethylamino tempamine). Both methods gave essentially the same result. The spin probe measurement was accomplished by adding 1 mM CAT1 to cells suspended in the various test solutions and pelleting them. The trapped CAT1 in the pellet was then measured and compared to the supernatant signal. The ratio gave the trapped volume fraction and ranged from 3–5%.

ESR measurements were made on an IBM ESR spectrometer, model #ER 200D-SRC, equipped with an IBM-AT and a Data Translation DT2800 series data acquisition board. Acquisition and analysis programs were developed using ASYST, a FORTH-based compiler and subroutine library package. Microwave power was 9.9 mW, klystron frequency was 9.78 GHz. Modulation amplitude was set to 1 gauss for calibration and static volume experiments. Although this value overmodulates the narrow Tempone spectral lines the signal to noise is improved by a factor of three when compared to modulation of 0.2. Further, correlation times obtained according to Mastro and Keith (1981) at either modulation agreed to within 10%. First derivative line heights with appropriate corrections were used for equilibrium volume determinations (*see* Calculation of Static Volumes Using Glycerol Calibration Curves). This was necessary because of the sensitivity of integrated spectra to errors from the small but finite quenched background, and peak asymmetries resulting from the high dielectric constants of the samples (Dalal, Eaton & Eaton, 1981).

Kinetic data were obtained with a computer-controlled stop-flow using either a vacuum aspirator or an Update Instruments syringe drive; the latter allows very precise control of mixing ratios and fluid velocity. Typically, equal volumes of cells and challenge solution were combined through a T-mixer, passed through the ESR sample volume consisting of a 1.0-mm i.d. quartz tube, and the flow stopped. Final hematocrits ranged from 7.5–10%. Fluid velocity was adjusted to 3.5–7 m/sec assuring turbulent mixing. Osmotic perturbations were effected by external sucrose or KCl. Cell and challenge solutions contained equal concentrations of chromium quencher (50 mM).

For kinetic experiments the volume relaxations are of principal concern rather than the absolute volumes. To increase signal to noise, 1–2 mM Tempone was present in cell and challenge solution, and the modulation amplitude chosen to maximize signal intensity without concern for maintaining accurate line shapes. To minimize viscosity-dependent signal changes, the midfield line was used to monitor water volume, and volume excursions were kept to about ±12% of isotonic volume. In general, no corrections to the kinetic data are then necessary.

To estimate the permeability of Tempone, its unidirectional influx was measured by mixing 1 mM probe in 75 mM KCl plus 50 mM quencher against cells suspended in the same media without probe. Under these conditions there is no cell volume change. The syringe drive was used to generate a flow rate of 680 cm/sec producing a signal about 35% lower than its final equilibrium value. The rate of relaxation was then used to estimate the Tempone permeability (*see* Results, Fig. 6).

Calculation of Static Volumes Using Glycerol Calibration Curves

The red cell internal water content was quantitated by comparing the spin probe line amplitudes in a quencher suspension of cells with an unquenched aqueous reference solution of the same total volume and number of spins. In principle with the external signal completely quenched, the remaining intracellular signal is then a measure of the internal volume. Since Tempone is a neutral probe its concentrations in the external and internal compartments will be equal making the number of spins per compartment proportional to their respective volumes. However, it is not possible to take a simple ratio of the quenched to unquenched signal to obtain the intracellular volume. The intracellular probe signal must be corrected for the effects of viscosity, changes in cavity Q, and filling factor. These effects are the result of the high internal cell hemoglobin which significantly raises intracellular viscosity and decreases the intracellular dielectric constant by replacing cell water. Our approach to this problem is empirical. Rather than attempt to sort out the individual contributions of these factors to the Tempone spectra inside the red cell, we simulated the spectral characteristics of the cell interior by measurements of probe spectra in water solutions of glycerol ranging from 0–90%. Glycerol was chosen because of its water solubility, moderate dielectric constant relative to water, and the ability to produce a broad range of viscosities which span the measured values of hemoglobin solutions (Chien, 1977).

We begin by noting that for a given concentration of probe, the volume W_{aq} of a simple aqueous solution is proportional to the number of spins and therefore to the height of the midfield peak $h_{o,aq}$ taken from that sample. Similarly in a suspension of cells, if the probe is in equilibrium, then the intracellular water volume W_i is proportional to the height of the corresponding midfield peak $h_{o,i}$ taken from the quenched spectrum of the cell suspension. It follows that

$$W_{aq} = k_{aq} h_{o,aq} \tag{1}$$

$$W_i = k_i h_{o,i} \tag{2}$$

where k_i and k_{aq} are constants of proportionality which depend on the medium. As we move from aqueous to intracellular media those factors (intracellular viscosity, Q, filling factor) that have the most significant influence on k also change the ratio $r = h_{+1}/h_o$ of the high to midfield peaks. For a convenient empirical calibration, we assume that these effects can be simulated by choosing a glycerol solution that has the same value of r as the intracellular sample. Strictly speaking, r is a function of the viscosity only; however, for glycerol and hemoglobin solutions their dielectric and viscosity properties are both functions of their concentrations. Therefore, changes in viscosity will be correlated with changes in dielectric constant. Thus, we may regard k as a function of r alone such that

$$k(r)_i = k(r)_g \tag{3}$$

where $k(r)_g$ is, by definition, the constant of proportionality relating W_g the volume of a glycerol-water mixture to its line height $h_o(r)_g$, i.e.,

$$W_g = k(r)_g h_o(r)_g. \tag{4}$$

The validity of Eq. (3) was tested by comparison of our final results for ESR estimations of cell water with wet-dry measurements on the same samples (*see* Results).

For calibrations, we use equal volumes of aqueous and glycerol mixture solutions so that $W_{aq} = W_g$. Using this condition together with Eqs. (1) and (4) yields

$$\frac{k_{aq}}{k(r)_g} = \frac{h_o(r)_g}{h_{o,aq}} \tag{5}$$

and using Eq. (3)

$$\frac{k_{aq}}{k(r)_i} = \frac{h_o(r)_g}{h_{o,aq}}. \tag{6}$$

The dependence of the right hand side of Eq. (6) on r can be evaluated from spectra of the glycerol reference solutions; it is plotted in Fig. 1. To expedite computations, an empirical polynomial function $f(r)$ has been fit to the data and is illustrated by the solid line.

$$\frac{k_{aq}}{k(r)} \approx a_0 + a_1 r + a_2 r^2 + a_3 r^3 + a_4 r^4. \tag{7}$$

Dividing Eq. (2) by Eq. (1), using Eq. (7), we arrive at the following final expression for W_i, the volume of cell water

$$W_i = \frac{1}{a_0 + a_1 r + a_2 r^2 + a_3 r^3 + a_4 r^4} \frac{h_o(r)_i}{h_{o,aq}} W_{aq}. \tag{8}$$

To summarize, the internal cell water for a particular sample is obtained as follows: (*i*) h_{+1}/h_o is measured to determine r, (*ii*) after adjusting for differences in instrument gain, Eq. (8) is used to calculate the total cell water. Dividing the latter by the number of cells in the sample gives the water volume per cell. For the highest accuracy allowance must be made for the volume

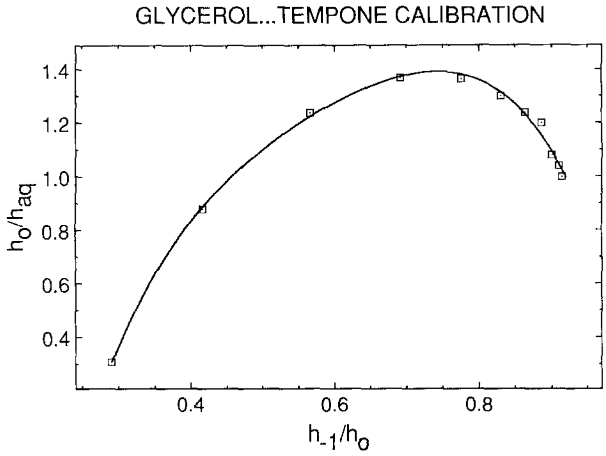

Fig. 1. Amplitude correction factor for midfield peak *versus* ratio of high field to midfield peak. Solid line given by polynomial fit discussed in text. ($y = -4.38 + 30.395x - 67.977x^2 + 74.082x^3 - 31.741x^4$; $r^2 = 0.996$)

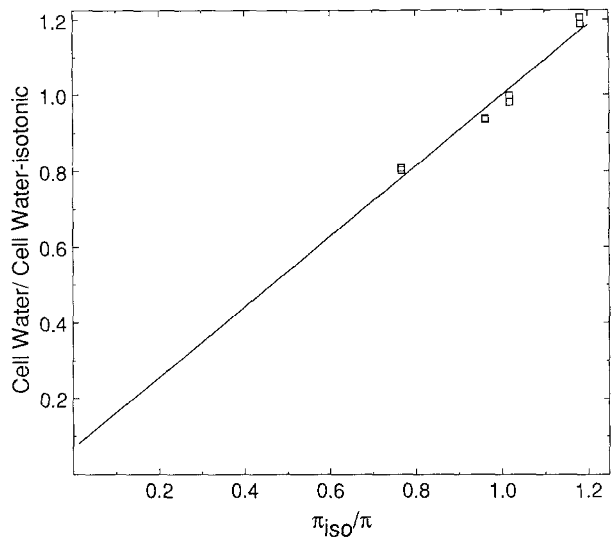

Fig. 2. Cell water *versus* the reciprocal of external osmolarity. Straight line fit used to determine parameter b_m from intercept. ($y = 0.0695 + 0.9304x$; $r^2 = 0.964$)

occupied by cell solids. The correction is required because the same total number of spins are added to cell suspensions and standards with the result that the probe will have a larger aqueous concentration in the cells. For most experiments the error amounted to no more than 4%, and was corrected from determination of the cell solids.

Kinetics of Water Transport

To analyze the osmotic transient experiments, we note that the spin probe is always used in small (tracer) quantities and makes no significant contribution to the osmotic pressure in either intra- or extracellular fluids. Let S_i and S_o denote the *amounts* of intra- and extracellular spin probe, W_i and W_o the intra- and extracellular water volumes, and let C_{mi} and C_{mo} denote the intra- and extracellular concentrations of impermeable solutes in Osm/cm^3, then

$$J_v = P_f V_w (C_{mi} - C_{mo}) \tag{9}$$

$$J_s = P_s\left(\frac{S_o}{W_o} - \frac{S_i}{W_i}\right) \tag{10}$$

where P_f and P_s are the filtration (osmotic water) and spin probe permeability coefficients (cm/sec), and V_w is the partial molar volume of water. To use these expressions, first note the data in Fig. 2 which shows the dependence of W_i on $1/C_{mi}$ over the range of cell volumes used in our transient experiments. It is conveniently described by a linear relation and can be used in Eq. (9) to replace C_{mi} in favor of W_i. Letting W_{iso} represent the isotonic intracellular water volume, obtained when cells are placed in isotonic medium with osmolarity C_{iso} (= 288 mOsm), this relation can be described by

$$C_{mi} = \frac{C_{iso} W_{iso}(1 - b_m)}{W - b_m W_{iso}} \tag{11}$$

where b_m is an empirical constant (=0.07 as determined by the straight line in Fig. 2). Further let A denote the surface area of the cell, then

$$AJ_v = \frac{dW_i}{dt}, \qquad AJ_s = \frac{dS_i}{dt}. \tag{12}$$

Finally, to simplify the analysis, we normalize W and S relative to isotonic conditions by using the following definitions (normalized values shown in lower case):

$$w_i = \frac{W_i}{W_{iso}},\ w_o = \frac{W_o}{W_{iso}},\ c_{mo} = \frac{C_{mo}}{C_{iso}},\ s_i = \frac{S_i}{S_{iso}},\ s_o = \frac{S_o}{S_{iso}}. \tag{13}$$

Substituting Eqs. (11), (12) and (13) into Eqs. (9) and (10) yields two equations for w_i and s_i

$$\frac{dw_i}{dt} = P_f V_w C_{iso}\left(\frac{A}{W_{iso}}\right)\left(\frac{1 - b_m}{w_i - b_m} - c_{mo}\right) \tag{14}$$

$$\frac{ds_i}{dt} = \frac{P_s A}{W_{iso}}\left(\frac{s_o}{w_o} - \frac{s_i}{w_i}\right). \tag{15}$$

In addition to the above we have the following two conservation expressions

$$w_o = w_T - w_i,\ s_o = s_T - s_i \tag{16}$$

where w_T and s_T are the total (extracellular + intracellular) water volume and total number of spins (normalized) in the sample.

Experiments are always performed with the spin probe initially in equilibrium; the initial conditions can be measured directly or calculated as:

$$\text{for } t = 0:\ w_i = b_m + \frac{1 - b_m}{c_{m,\mathrm{inc}}},\ s_i = \frac{w_i}{w_T} s_T \tag{17}$$

where $c_{m,\mathrm{inc}}$ denotes the value of c_m in the incubation medium where the cells had equilibrated just prior to mixing (i.e., for $t < 0$).

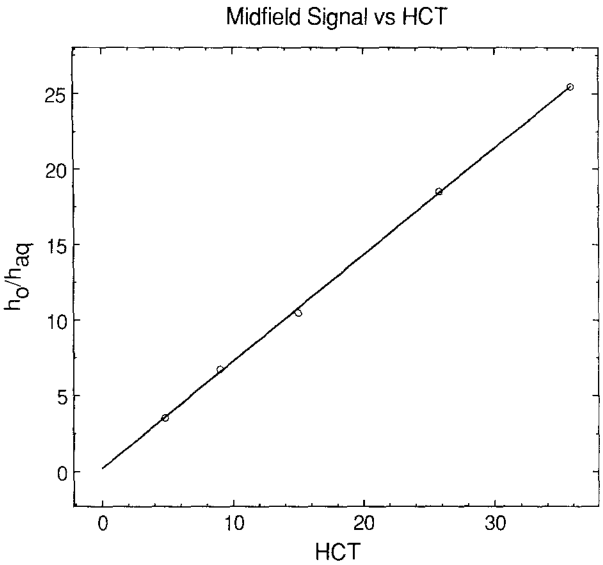

Fig. 3. Midfield signal $h_{o,i}$ relative to control $h_{o,aq}$ *versus* RBC hematocrit. ($y = 0.207 + 0.707x$; $r^2 = 1.00$)

Equations (14) and (15), together with Eqs. (16) and (17), were numerically integrated using a 4th-order Runge-Kutta algorithm. Letting P_f vary within the useful range of 0.005 to 0.04 cm sec^{-1}, families of solutions were generated and compared to corresponding experimental results. Our estimate of P_f is then obtained by the best fit (least squares deviation) with the experimental data. Implementation of this procedure requires a prior estimate of A which was assumed equal to 1.37×10^{-6} cm^2 (Jay, 1975). Values for other parameters were measured directly on the cells under investigation as described in Materials and Methods. Our best estimate for W_{iso} was 59.2×10^{-12} cm^3 giving $A/W_{iso} = 2.3 \times 10^4$ cm^{-1}, an estimate equal to the figures obtained by Brahm (1982) and by Wieth et al. (1974). Combining b_m from Fig. 2 with the solid volume fraction we estimate a value for the "osmotic dead space" of 0.41 in good agreement with literature values which plot the whole cell volume rather than cell water (Macey & Brahm, 1989).

Results

Signal *vs.* Hematocrit

A very simple test of the ESR method for determination of red cell volumes is illustrated in Fig. 3 which plots $h_{o,i}/h_{o,aq}$ in percent *versus* the hematocrit for conditions of constant external osmotic activity (312 mOsm). In this case, the spectral characteristics associated with the intracellular medium are held constant. For hematocrits up to 35%, the peak height follows the hematocrit in a precisely linear fashion with a slope of 0.707 ($r^2 = 1.00$) and y-intercept effectively zero (0.2%). This experiment clearly demonstrates the simple proportionality of the ESR signal on intracellular volume and supports the assumption that $W_i = k_i h_{o,i}$, Eq. (2).

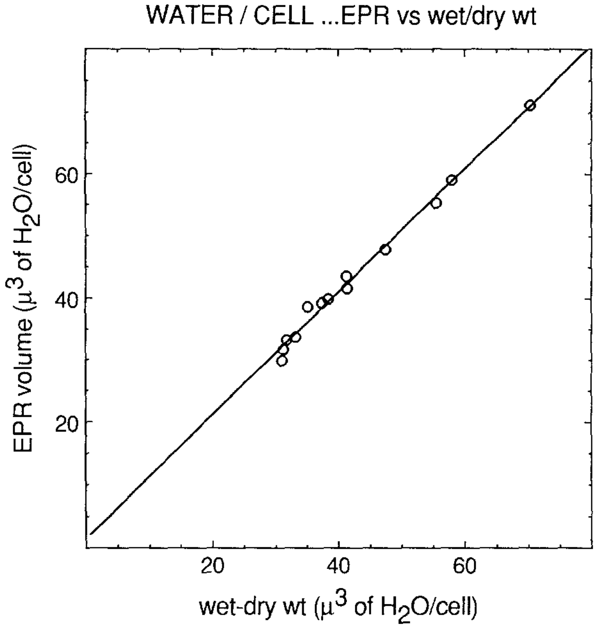

Fig. 4. Comparison between ESR measured water per cell *versus* wet-dry method on corresponding samples of blood. Each point is the mean of duplicate samples with the largest deviation from the mean of <1%. ($y = 1.3481 + 0.992x$; $r^2 = 0.99$)

Cell Volume *vs.* Osmotic Strength: ESR *vs.* Wet-Dry Weight

A more useful and critical test of the accuracy of the ESR volume determination was made by measuring the volume of water per cell using both ESR and the wet-dry weight method on the same samples of blood. Figure 4 compares the water volume per cell determined by both methods when the osmolalities were varied from 243 to 907 mOsm. In each sample, quencher and external chloride were held constant while the osmolalities were increased with sucrose. Ideally, the results of the two methods when plotted against each other will have a slope of 1 with an intercept of zero. This is amply borne out by the regression line shown in the figure, and argues convincingly for the correspondence of the two methods ($y = 1.3481 + 0.992x$; $r^2 = 0.99$). In addition, the legitimacy of using the glycerol calibration is successfully confirmed with the average deviation between the two methods $1.5 \pm 0.5\%$.

Intracellular Viscosity *vs.* Medium Osmolality

Figure 5 plots the intracellular red cell microviscosity obtained from the Tempone rotational correlation time *versus* the external osmotic activity. The cell microviscosities were obtained by first constructing a calibration plot of the known viscosities

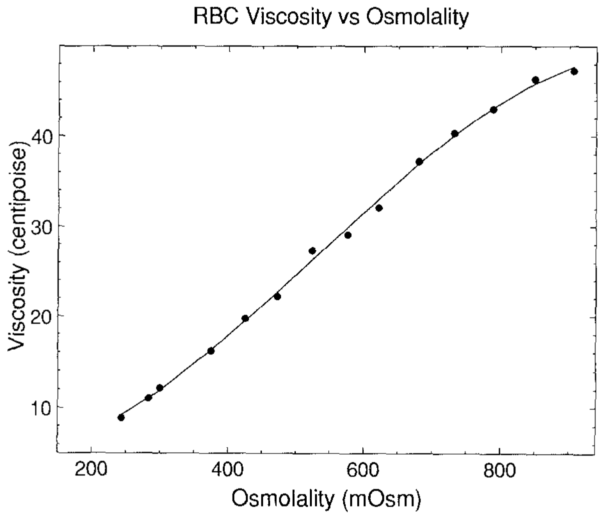

Fig. 5. Estimated RBC intracellular viscosity *versus* external osmotic activity. $T = 21°C$

of the glycerol mixtures (Wolf, Brown & Prentiss, 1972) *versus* their measured Tempone correlation times. The cell correlation times then give the equivalent glycerol viscosities. Values range from 9–47 centipoise at a temperature of 21°C.

Tempone Reduction by Red Cells

Red cells contain spin probe reducing components (Eriksson et al., 1986). We commonly observe a decay time of 40–60 min which introduces a fractional error of less than 1% in the volume measurement as long as readings are taken within 1–2 min of mixing. In cases where this is objectionable 5 mM ferricyanide added on top of the chromium quencher largely eliminates probe reduction. However, ferricyanide is also capable of oxidizing sensitive sulfhydryl groups and may be unsuitable in some studies.

Kinetics Results

The kinetic analysis of volume relaxation experiments requires an estimate of the Tempone permeability. For this purpose, we employed the Update Instruments syringe drive at a fluid velocity of 680 cm/sec to measure the rate of influx of Tempone with cells at constant volume. At this flow velocity the initial signal drops 35% below its equilibrium value. Figure 6*a* shows a comparison between the Tempone influx with no cell volume change and a typical water relaxation for cells that are swelling. Figure 6*b* shows the same Tempone influx but with the time scale expanded by a factor of 10. Clearly the Tempone response is much faster; fitting the time constant 15 msec after initiation of the relaxation gives a value of 17 msec which is 15–20 times faster than for normal red cell osmotic response. The early *S*-shape part of the curve was not used due to the finite stopping time of the syringe drive estimated to range from 4–6 msec by the manufacturer. (The finite permeability of Tempone is explicitly accounted for in the analysis of transient volume changes described later in this section).

Figure 7 shows a hypotonic, a hypertonic, and an isosmotic challenge of the same batch of blood. Cells were initially suspended either in 50 mM KCl plus 50 mM quencher (solution A: mOsm = 252) or 100 mM KCl plus 50 mM quencher (solution B: mOsm = 330). The former cells were challenged with solution B and the latter with A in the presence of 1 mM Tempone. Consequently, cells reach the same final tonicity (288 mOsm) in each curve. The magnetic field was set at the midfield peak resonance of Tempone. Water volume excursions are about 12% for both curves. Notice that the isosmotic curve is flat demonstrating that the ESR measurement is free of mechanical or electronic artifacts. In contrast, light scattering experiments are complicated by large optical artifacts occurring in the first 200–300 msec which is close to the water relaxation time itself (Farmer & Macey, 1970; Terwilliger & Solomon, 1981; Mlekoday et al., 1983). This creates significant difficulties in interpreting and calibrating light scattering data. Data shown in the figures allows usable volume measurements to be obtained within 30 msec after mixing without resorting to baseline subtraction. This represents a five to 10-fold improvement over light scattering. Further improvement can be anticipated as dead times, stopping times and window size are minimized.

Figure 8*a* and *b* show nonlinear least squares fit of Eqs. (14) and (15) for the swell and shrink data in Fig. 7 as described in Kinetics of Water Transport subsection of Materials and Methods. The corresponding water permeabilities obtained from the fits are 0.029 and 0.030 cm/sec for the swell and shrink, respectively. These figures are on the high end of values reported in the literature which generally average around 0.020 cm sec^{-1} (Macey, 1979; Macey & Brahm, 1989), but values of 0.028 and 0.032 cm sec^{-1} have been reported by Terwilliger and Solomon (1981) and by Galey (1978). Although it is tempting to ascribe the high permeability reported here to the fact that the ESR method allows analysis of the earlier, more rapidly changing portions of the osmotic relaxation, it may only reflect different values assumed for cell area; these are not always explicitly stated.

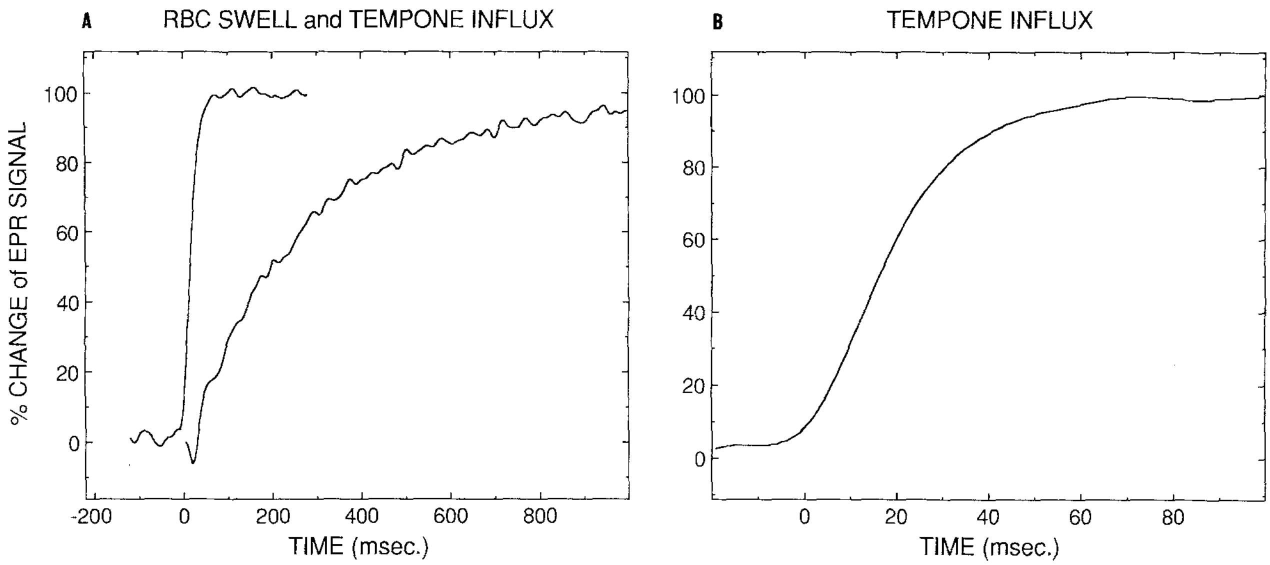

Fig. 6. (*A*) Comparison of typical water influx *versus* Tempone influx. (*B*) Tempone influx with the time scale expanded 10 times. (Data digitally filtered to remove high frequency noise)

The uptake and release of Tempone by the cells lags slightly behind the water. This lag is directly accounted for in our analysis and computation of P_f. However, a comparison of theoretical curves for W and S shows that the lag is very slight. Figure 9 shows computer simulations which compare the expected ESR signal and the calculated water volume in a shrink experiment assuming normal water permeability. The computer volume change is the solid line and the theoretical ESR signal the dashed line. Clearly, the differences are minor with a slight phase lag shown in the Tempone response. These results suggests that for most studies the Tempone curve could be substituted for water (i.e., as if the permeability of Tempone is infinite).

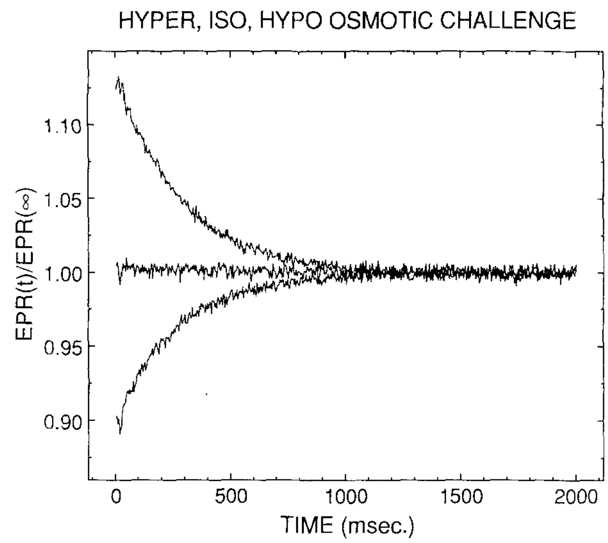

Fig. 7. Shrink, swell and iso-volumetric kinetic curves. Midfield signal average of nine repetitions. Instrument time constant set to 1 msec. Modulation amplitude = 2.5 and gain = 1.6×10^{4}. Final tonicity = 288 mOsm for each curve

Discussion

Equilibrium Volumes

We have shown that with use of Tempone, the accuracy of the ESR method is fully comparable to other standard techniques for measuring red cell equilibrium volumes (Fig. 4). In addition, the red cell intracellular microviscosity can be determined at the same time. Tempone was originally used as a volume probe because its narrow intrinsic line widths are effectively broadened by low concentrations of paramagnetic quenching agents. Thus, the osmotic effects of the quenching agents are minimized, making it easier to control cell volume (Mehlhorn et al., 1982). In the erythrocyte at normal hematocrits, this advantage translates into effective quenching of the extracellular Tempone signal with as little as 15 mM of Mn-EDTA (*data not shown*).

The benefits of lower quencher concentrations required for Tempone are partially offset by its spectral sensitivity to other influences such as viscosity, spin-spin interactions and power saturation effects. Furthermore, quantitative volume measurements using ESR for biological specimens are in

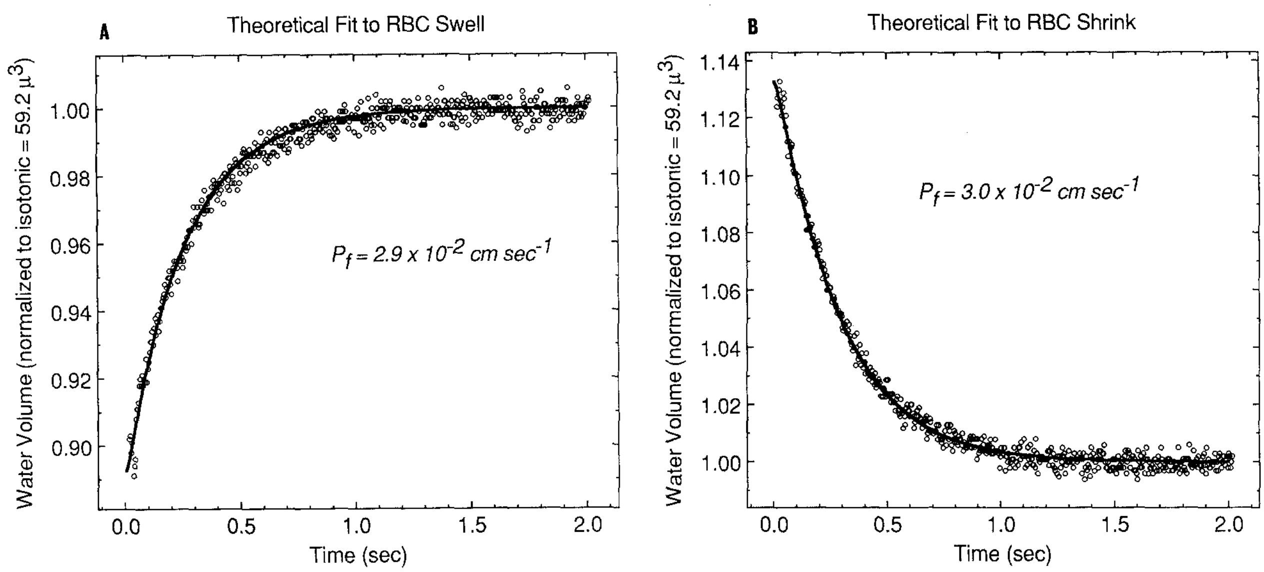

Fig. 8. Nonlinear fits for (*A*) swell and (*B*) shrink curves from Fig. 7

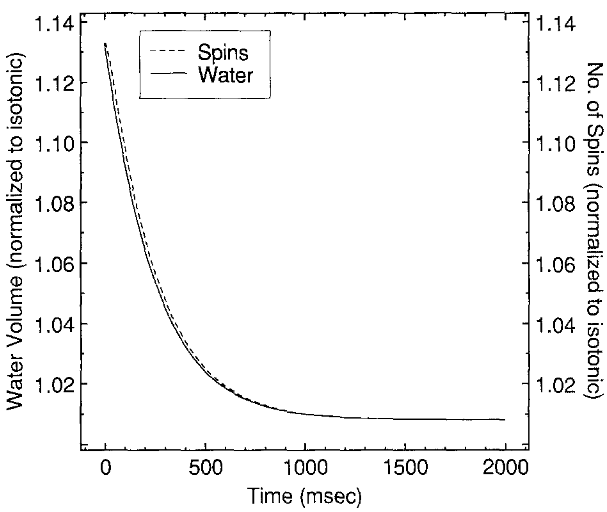

Fig. 9. Comparison of simulated shrink data for water volume and expected ESR signal

general complicated by changes in probe spectral properties, resulting from spectrometer sensitivity variations related to cavity Q, and filling factor. In the present study, the various factors affecting the Tempone signal are accounted for empirically by simulating the intracellular environment with glycerol solutions.

The high intracellular red cell viscosity causes a decrease in h_{-1}/h_o associated with reduced rates of tumbling, and a concomitant increase in the rotational correlation time (Daveloose et al., 1983; Morse, 1985). According to the Kivelson theory, increasing viscosity should increase the width and decrease the height of each ESR line (Kivelson, 1960); this is only true if there is no line broadening from collisional self-quenching. Collisional self-quenching is reduced in high viscosity media and leads to line narrowing and an increase in amplitude (Mastro & Keith, 1981). This effect may be compensated by using low concentrations of probe at the expense of signal to noise. Our use of 200 μM Tempone in standards and samples was a reasonable compromise. However, a comparison of line widths between water and 50% glycerol (viscosity ~ RC at normal volume) found a 7% narrowing of h_o which translates into about a 14% increase in line amplitude; since $k = 1.32$ for this glycerol concentration about half of the amplification appears to result from the reduction in collisional self-quenching.

The replacement of sample water by hemoglobin decreases the sample dielectric constant which oppositely affects both cavity Q and filling factor. Specifically, these effects apply to the 9.78 GHz out-of-phase and in-phase dielectric constants ε'' and ε' (Dalal et al., 1981). A lower ε'' increases Q which increases the signal amplitude. The "lens effect" which depends on ε' is decreased which reduces the filling factor and lowers signal amplitude. The first effect is the larger of the two so that a net amplification results of the spin probe signal. The total effect of all the processes kept the value of k_g for h_o above 1 throughout the 5–90% range of the glycerol mixtures tested (Fig. 1).

With the current apparatus static measurements on samples as small as 5 μl of cell water are easily accomplished. We anticipate that additional improvements will be possible using a loop gap resonator currently under study. This should make it possible to measure water volumes in 0.2 μl of cells. The ability to measure the intracellular microviscosity and cell water in a single measurement suggests the use of ESR to evaluate cells in simulated environments like those in the kidney. Cells traversing the kidney vasa recta are transiently subject to severe shrinkage because of the very high osmotic activity. Under such circumstances the viscosity can increase greatly, reduce cell deformability, and increase the resistance of cells to flow through the vasa recta. It has been proposed that facilitated urea transport is important for preventing red cells lysis upon exiting the kidney (Macey & Yousef, 1988), but it may also act to moderate viscosity increases that could adversely affect the ability of red cells to negotiate the vasa recta.

Kinetic Measurements

The measured osmotic water permeability, 0.029–0.030 cm sec^{-1}, is within the range of values obtained using light scattering methods, and it is also consistent with novel estimates of P_f based on urea efflux studies while cells undergo osmotically induced volume changes (R.I. Macey and J. Brahm, *in preparation*). Taken together, these results remove much of the uncertainty about osmotic permeability and clearly establish the assertion that $P_f > P_d$.

The ESR method is much superior to light scattering because its calibration is simple and does not require a correction for changes in the refractive index every time the composition of the medium is altered (Terwilliger & Solomon, 1981; Mlekoday et al., 1983). More importantly, the first 250 msec of a light scattering trace is generally contaminated by mixing artifacts which probably arise from vortex patterns that are dissipated upon stopping the flow, or from transient mixing movements introduced by rapid injection devices (Farmer & Macey, 1970; Mlekoday et al., 1983). Efforts to circumvent these problems by sphering the cells with lysolecithin (Mlekoday et al., 1983) or by subtraction of baselines obtained by isosmotic mixing are neither totally successful, nor free from other assumptions. The former assumes that the chemical treatment and corresponding shape change have no effect on the process under investigation, whereas the latter assumes that the mixing transient obtained under control isosmotic mixing is identical to the artifact seen under experimental conditions.

These mixing transients are absent from ESR traces which respond only to changes in the number of intracellular spin signals and not to cell orientations. The ability of the stopped-flow ESR method to follow rapid volume changes within the first few milliseconds after mixing opens the way to obtain unambiguous measurements of net fluxes, permeabilities, reflection coefficients and other transport parameters of rapidly permeating solutes like urea. Further, use of the loop gap resonator will make measurements on very small sample sizes feasible.

This work was supported by NIH grants GM18819, HL37593, HL20985, and AG48018.

References

Adorante, J.S., Cala, P.M. 1987. Activation of electroneutral K^+ flux in *Amphiuma* red blood cells by N-ethylmaleimide: Distinction between K^+/H^+ exchange and KCl cotransport. *J. Gen. Physiol.* **90:**209–227

Anzai, K., Higashi, K., Kirino, Y. 1988. Rapid determination of internal volumes of membrane vesicles with electron spin resonance-stopped flow technique. *Biochim. Biophys. Acta* **937:**73–80

Beaudoin, G., Mizukami, H. 1978. Correlation times of 2,2,6,6-tetramethyl piperdone-N-oxyl (Tempone) in solutions of hemoglobin A and hemoglobin B. *Biochim. Biophys. Acta* **532:**41–47

Bookchin, R.M., Balazs, T., Landau, L.C. 1976. Determinants of red cell sickling. Effects of varying pH and of increasing intracellular hemoglobin concentration by osmotic shrinkage. *J. Lab. Clin. Med.* **87:**597–616

Brahm, J. 1982. Diffusional water permeability of human erythrocytes and their ghosts. *J. Gen. Physiol.* **79:**791–801

Chien, S. 1977. Rheology of sickle cells and erythrocyte content. *Blood Cells* **3:**283–303

Dalal, D.P., Eaton, S.A., Eaton, G.R. 1981. The effects of lossy solvents on quantitative EPR studies. *J. Magn. Res.* **44:**415–428

Daveloose, D., Fabre, G., Berleur, F., Testylier, G., Leterrier, F. 1983. A new spin label method for the measurement of erythrocyte internal microviscosity. *Biochim. Biophys. Acta* **763:**41–49

Eriksson, U.G., Tozer, T.N., Sosnovsky, G., Lukszo, J., Brasch, R.C. 1986. Human erythrocyte membrane permeability and nitroxyl spin-label reduction. *J. Pharm. Sci.* **75:**334–337

Farmer, E.E.L., Macey, R.I. 1970. Perturbation of red cell volume: Rectification of osmotic flow. *Biochim. Biophys. Acta.* **196:**53–65

Finkelstein, A., Rosenberg, P.A. 1979. *In* Single-file transport: Implications for ion and water movement through gramicidin A channels. C.F. Stevens and R.W. Tsien, editors. pp. 73–88. Raven, New York

Galey, W.R. 1978. Determination of human erythrocyte membrane hydraulic conductivity. *J. Membrane Sci.* **4:**41–49

Hubbell, W.L., Froncisz, W., Hyde, J.S. 1987. Continuous and stopped flow EPR spectrometer based on a loop gap resonator. *Rev. Sci. Instrum.* **58:**1879–1886

Jay, A.W.L. 1975. Geometry of the human erythrocyte. *Biophys. J.* **15:**205–222

Kivelson, D. 1960. Theory of ESR linewidths of free radicals. *J. Chem. Phys.* **33:**1094–1107

Levitt, D.G., Subramanian, G. 1974. A new theory of transport for cell membrane pores. II. Exact results and computer simulation (molecular dynamics). *Biochim. Biophys. Acta* **373:**132–140

Macey, R.I. 1979. Permeability of red cells to water and nonelectrolytes. *In:* Transport Across Biological Membranes. G. Giebisch, D.C. Tosteson, and H.H. Ussing, editors. pp. 1–58. Springer-Verlag, Berlin–Heidelberg–New York

Macey, R.I., Brahm, J. 1989. Osmotic and diffusional water permeability in red cells: Methods and interpretations. *In:* Water Transport in Biological Membranes. G. Benga, editor. pp. 25–40. CRC Press, Boca Raton (FL)

Macey, R.I., Karan, D.M., Farmer R.E.L. 1972. Properties of water channels in human red cells. *In:* Biomembranes. F. Kreuzer and J.F.G. Slegers, editors. pp. 331–334. Plenum, New York

Macey, R.I., Yousef, L.W. 1988. Osmotic stability of red cells in renal circulation requires rapid urea transport. *Am. J. Physiol.* **254:**C699–C674

Mastro, A.M., Keith, D.K. 1981. Spin label viscosity studies of a mammalian cell cytoplasm. *In:* The Transformed Cell. pp. 327–345. Academic, New York

Mehlhorn, R.J., Candau, P., Packer, L. 1982. Measurements of volumes and electrochemical gradients with spin probes in membrane vesicles. *In:* Methods in Enzymology. pp. 751–761. Academic, New York

Mlekoday, H.J., Moore, R., Levitt, D.G. 1983. Osmotic water permeability of the human red cell. *J. Gen. Physiol.* **81:**213–220

Morse, P.D. 1985. A comparison of the spin labels MAL-3 and Tempamine for measuring the internal microviscosity of human red cells. *Biochim. Biophys. Acta.* **844:**337–345

Moura, T.F., Macey, R.I., Chien, D.Y. Karan, D., Santos, H. 1984. Thermodynamics of all-or-none water channel closure in red cells. *J. Membrane Biol.* **81:**105–111

Paganelli, C.V., Solomon, A.K. 1957. The rate of exchange of tritiated water across the human red cell membrane. *J. Gen. Physiol.* **41:**259–277

Terwilliger, T.C., Solomon, A.K. 1981. Osmotic water permeability of human red cells. *J. Gen. Physiol.* **77:**549–570

Vistnes, A.I., Puskin, J.S. 1981. A spin label method for measuring internal volumes in liposomes or cells, applied to Ca-dependent fusion of negatively charged vesicles. *Biochim. Biophys. Acta.* **644:**244–250

Wieth, J.O., Funder, J., Gunn, R.B., Brahm, J. 1974. Passive transport pathways for chloride and urea through the red cell membrane. *In:* Comparative Biochemistry and Physiology of Transport. L. Bolis, K. Bloch, S.E. Luria, and F. Lynem, editors. pp. 317–337. North-Holland, Amsterdam

Williams, A.R., Morris, D.R. 1980. The internal viscosity of the human erythrocyte may determine its lifetime in vivo. *Scand. J. Haematol.* **24:**57–62

Wolf, A.V., Brown, M.G., Prentiss, P.B. 1972. Concentrative properties of aqueous solutions. *In:* CRC Handbook of Chemistry and Physics. R.C. Weast, editors. pp. D191–192. Chemical Rubber Co., Cleveland (OH)

Received 14 June 1989; revised 27 September 1989